Ion Mobilities, Transference Numbers, and Inverse Haven Ratios of **Polymeric Ionic Liquids**

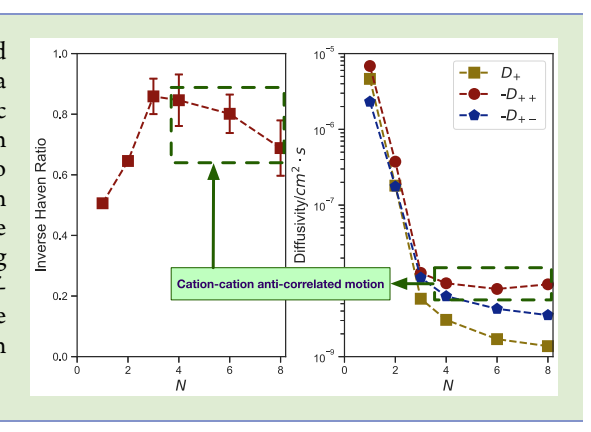
Zidan Zhang, Bill K. Wheatle, Iakub Krajniak, Iordan R. Keith, and Venkat Ganesan,

[†]McKetta Department of Chemical Engineering, University of Texas at Austin, Austin, Texas 78712, United States

Supporting Information

Downloaded via UNIV OF TEXAS AT AUSTIN on July 6, 2020 at 21:13:58 (UTC). See https://pubs.acs.org/sharingguidelines for options on how to legitimately share published articles.

ABSTRACT: We probe the ion mobilities, transference numbers, and inverse Haven ratio of ionic liquids and polymerized ionic liquids as a function of their molecular weight using a combination of atomistic equilibrium and nonequilibrium molecular dynamics simulations. In contrast to expectations, we demonstrate that the inverse Haven ratio increases with increasing degree of polymerization (N) and then decreases at larger N. For a fixed center of mass reference frame, we demonstrate that such results arise as a consequence of the strong cation-cation correlated motions, which exceed (in magnitude) the selfdiffusivity of cations. Together, our findings challenge the premise underlying the pursuit of pure polymeric ionic liquids as high transference number, single-ion conducting electrolytes.



he pursuit of high transference number polymer electrolytes has turned its focus to single-ion conductors (SICs) in which either anions or cations are immobilized by coupling to the polymer backbone. 1-6 However, despite many seminal developments in this regard, it has been a challenge to retain high cation (anion) mobility while still tethering the anion (cation) to the polymer. Indeed, due to the low polarity of the polymer, strong ion pairing interactions manifest and render the free ions relatively immobile, leading to low conductivities that nullify the advantages of a fixed-ion electrolyte. To overcome such challenges, attention has turned toward polymeric ionic liquids (polyILs), which are comprised of ionic liquids (ILs) as their repeating units.8-13 PolyILs represent a class of SICs that combine the unique physicochemical and ion transport characteristic of ILs with the enhanced mechanical properties of polymers. 14-17 More pertinently, due to the weaker/delocalized electrostatic ionpair interactions accompanying such materials, polyILs are expected to possess high conductivities and lower glasstransition temperatures, even at high charge densities. 18-2

The significant interest in polyILs s and SICs arise from some hypotheses regarding ion motion in such systems. Specifically, the ions bound to the polymer chain are envisioned to be relatively immobile at the probed temperature. As a consequence, correlated motion of the free and bound ions have been hypothesized to be negligible. Such an assumption justifies the use of Nernst–Einstein (NE) equation for the conductivity of the material (for the case in which the free ions are anions and the polymerized ion is a cation): ^{24,25}

$$\sigma_{\rm NE} = \frac{\rho}{k_{\rm B}T} \left[\frac{1}{N+1} z_{+}^{2} D_{+} + \frac{N}{N+1} z_{-}^{2} D_{-} \right] \tag{1}$$

where ρ is the number density of the total charge carriers, $k_{\rm B}$ is the Boltzmann constant, T is the temperature, N is the degree of polymerization, z_{\perp} is the charge of each polymer chain, and z_{-} is the magnitude of the charge of anion $(z_{+} = N \cdot z_{-})$. D_{+} and D_ are the self-diffusivities of cation and anion, respectively (cf. SI, section S1). Under such an assumption, the inverse Haven ratio H^{-1} , defined as

$$H^{-1} = \frac{\sigma}{\sigma_{\rm NE}} \tag{2}$$

where σ represents the true conductivity of the material, is expected to be close to unity. Further, an "ideal" transference number can be expressed based on the current carried by the anion relative to the total current:

$$t_{-}^{NE} = \frac{z_{-}D_{-}}{z_{-}D_{-} + z_{+}D_{+}}$$
(3)

Using eq 3 in conjunction with the hypothesis that the polymerized ion is expected to possess low mobility leads to the expectation that polyILs can serve as high transference number electrolytes.

Recent studies have raised questions on the validity of the above hypotheses underlying the pursuit of polyILs. In the context of ionic liquids, there have been a number of studies highlighting the role of dynamical ion correlations and its importance in influencing conductivity of such materials.^{26–28} Recently, Wieland et al. demonstrated the importance of

Received: November 18, 2019 Accepted: December 26, 2019 Published: December 31, 2019

[‡]Independent researcher, os. Kosmonautow 13/56, 61-631 Poznan, Poland

ACS Macro Letters

Letter

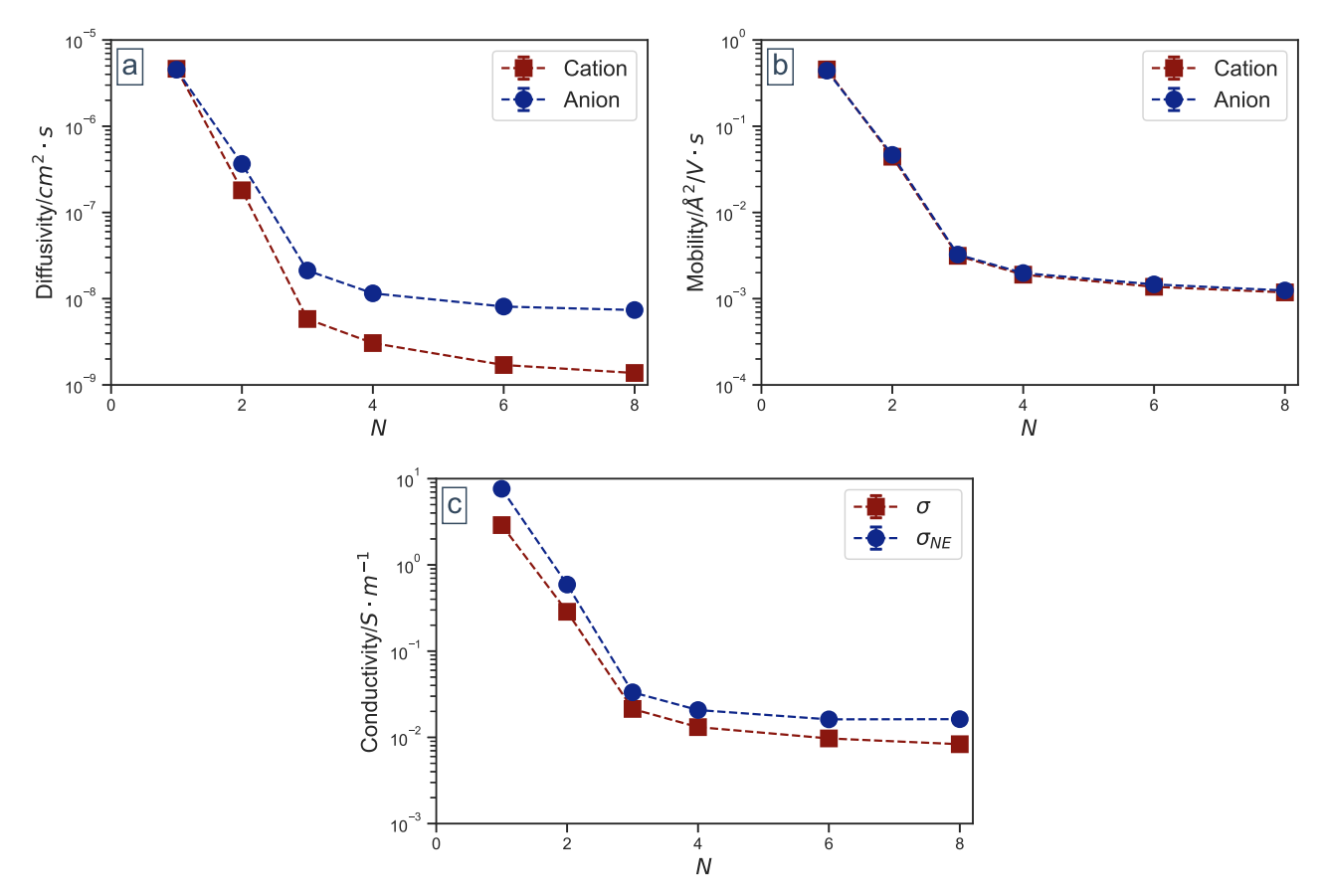


Figure 1. (a) Diffusion coefficient, (b) ionic mobility, and (c) Nernst–Einstein and true conductivities as functions of the degree of polymerization *N*.

similar dynamical ion correlations in polyILs by reporting that the inverse Haven ratio H^{-1} decreases monotonically with increasing degree of polymerization (N). However, despite the initial report of their observations, the physical mechanisms underlying their observations are still unresolved. Such experimental reports motivate the two questions we address in this study: (1) "What are the Haven ratios and ideal transference numbers of polyIL materials?" (2) "What is the role of the ion dynamical correlations in influencing transport in polyIL materials?" We note that resolution of these issues is critical to the foundational premise underlying the pursuit of SICs and polyILs as means to overcome concentration polarization effects in batteries.

In this work, we used atomistic molecular dynamics (MD) simulations to probe the transference numbers and inverse Haven ratios spanning the spectrum from ILs to polyILs. Specifically, we considered the system of 1-butyl-3-methylimidazolium hexafluorophosphate ILs ([BmIm]+[PF6]-) and quantified the influence of N on the transference number and $H^{-1.30-32}$ We characterized the ionic self-diffusivities D_{-} and D_{+} using the mean-squared displacement of the ions. Further, by using a nonequilibrium simulation approach involving the use of electric fields, we obtained the true ionic conductivity. The latter approach, while more computationally intensive compared to equilibrium approaches (due to the need to simulate multiple field strengths to probe the linear response regime), avoids the computational difficulties accompanying the equilibrium calculations. Explicitly, in our simulations, the ionic mobilities are obtained in the linear response regime as

$$\mu_i = \frac{\langle v \rangle_i}{E} \tag{4}$$

where $\langle v \rangle$ is the drift velocity of ion species i (i = + or -), and E is the strength of the external field. The individual ionic contributions to the conductivity are then obtained as $\sigma_i = z_i c_i \mu_i$, where z_i and c_i denote the charge and number densities of charge carrier i. The true conductivity is the summation of all individual conductivities and can be obtained as $\sigma = \sum_i \sigma_i$. Using the true conductivity σ and eq 2, we obtain the inverse Haven ratio for our materials.

As an aside, we note that since the center of mass frame of reference is stationary, the "true" transference number (t_{-}) for systems consisting only a pair of cation and anion is a constant and independent of N. This feature has been discussed in literature for the analogous case of single molten salts, and it has been concluded that true transference numbers are not meaningful for characterizing the performance of such materials. Explicitly, the stationarity of the center of mass requires that the mobilities of the ions to be inversely proportional to their molar masses, and hence 34

$$t_{-} = \frac{M_{\rm BmIm^{+}}}{M_{\rm PF_{6}^{-}} + M_{\rm BmIm^{+}}} \tag{5}$$

where M_i are the molar masses of species $i.^{35,36}$ Using $M_{\rm PF_6^-}=144.964$ and $M_{\rm BmIm}^+=139.221$ (or 151.232 for the repeating unit of polyBmIm) g/mol, which yields $t_-=0.49$ (or 0.51 for polyBmIm).

To maintain brevity of the text, we relegate most of the simulation details to the SI, section S2. In brief, we use classical

ACS Macro Letters Letter

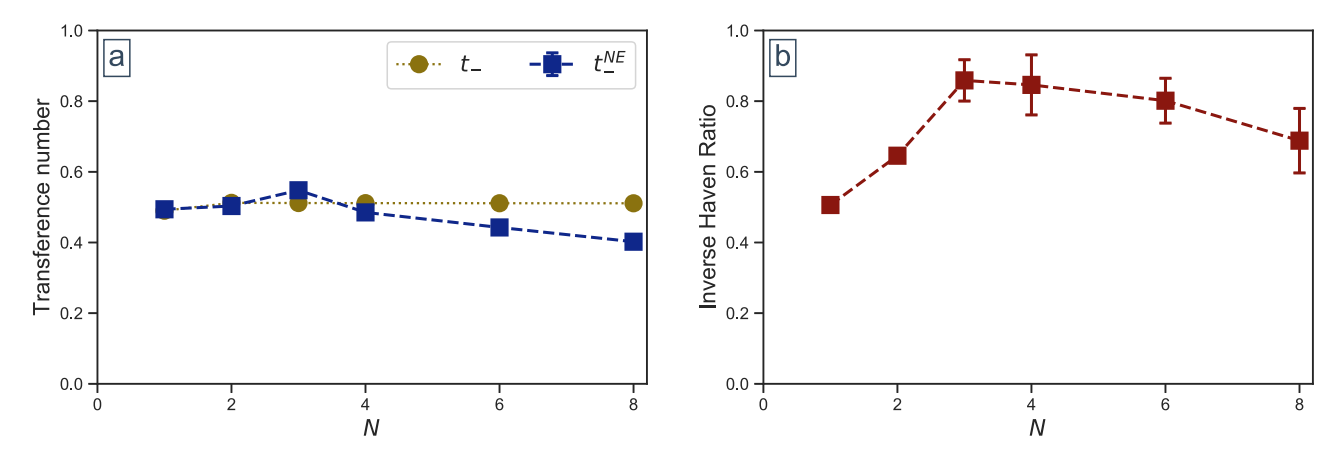


Figure 2. (a) The "ideal" transference number t_{-}^{NE} (dashed square, cf. eq 3) and the "true" transference numbers t_{-} (dotted circle, cf. eq 5); (b) The inverse Haven ratio H^{-1} .

MD simulations that include all intramolecular bonds, angles, dihedrals, impropers interactions, and nonbonded interactions for the calculation of potential energy function. The force field parameters are extracted from the optimized OPLS-all atom (OPLS-AA) force field set³⁷ that have been successfully used in our previous studies.^{30,32,38} We used simulations extending to 400 ns for obtaining the diffusivity of cations and anions (except for the monomer and dimer systems in which simulations of 30 and 60 ns were used respectively). Two methods for fitting the diffusivity coefficient from mean square displacement (MSD) were employed and compared, and both methods converge to the same results discussed below (cf. SI, sections \$3.1 and \$3.2). For the nonequilibrium MD simulation, 39-41 the strength of the external electric field was varied between 0.001 to 0.010 V/Å with an increment of 0.001 V/Å. We only use the first eight points for fitting the drift velocity $\langle v \rangle_i$ with the center of mass as the reference frame (cf. SI, section S3.3).

Figure 1a displays the results of diffusion coefficient for the anion and cation as a function of degree of polymerization N. It can be seen that the diffusivity of both anion and cations decrease rapidly in transitioning from monomer to trimers. However, for N > 3, we observe that the decrease becomes less pronounced. In Figure 1b, we show the mobility derived from the linear response regime under the external fields. We observe that the trends for mobility are similar to those seen for the diffusion coefficients. In accord with the discussion relating to eq 5 and the magnitude of the transference numbers being identically equal to 0.49 (or 0.51 for polyILs) for our system, we observe that the magnitude of mobility for cation is comparable to that of the anions.

By combining the results shown in Figure 1a,b, the ideal conductivity $\sigma_{\rm NE}$ and the true conductivity σ can be calculated, and the results are shown in Figure 1c. We observe that the difference between $\sigma_{\rm NE}$ and σ first decreases and increases again later with increasing N. These results are suggestive of nonmonotonic behavior for the inverse Haven ratio H^{-1} .

Figure 2a and b display the results for the ideal anionic transference number $t_-^{\rm NE}$ and the inverse Haven ratio H^{-1} , respectively, as functions of N. As discussed in the first paragraph, interest in polyILs (and the general class of SICs) arises from the promise of high (almost unity) ideal transference numbers due to the immobilization of one of the ions. In contrast, our results demonstrate the surprising result that ideal transference numbers of polyILs to be around

0.5 and decrease (slightly) with increasing N at large N. Moreover, the inverse Haven ratios also indicate nontrivial characteristics. Specifically, we observe that in transitioning from monomeric ILs to polyILs, H^{-1} initially increases with N, signifying a decreasing contribution to the conductivity arising from the correlated motion of distinct ions. However, beyond a critical N, we see that the H^{-1} again decreases, signifying an increasing contribution of the correlated motion of distinct ions to the overall conductivity.

To understand the microscopic origins of the results presented in Figure 2, we turn to a closer examination of the correlations in the dynamics of different ions. Toward this objective, we first break down explicitly the different contributions to the conductivity as

$$\sigma = \sigma_{-} + \sigma_{+} + \sigma_{--} + \sigma_{++} + 2\sigma_{+-} \tag{6}$$

in which $\sigma_- = (\rho e^2/k_B T)x_-z_-^2D_-$ and $\sigma_+ = (\rho e^2/k_B T)x_+z_+^2D_+$ are, respectively, the conductivity contributions arising from the anions and cations in the framework in which the ions are moving in an uncorrelated manner. The other terms above, σ_{--} , σ_{++} , and σ_{+-} , represent the conductivity contributions arising, respectively, from distinct anion—anion, distinct cation—cation, and cation—anion correlated motions. In turn, these contributions can be related to distinct diffusivities as $\sigma_{--} = (\rho e^2/k_B T)x_-^2z_-^2D_{--}$; $\sigma_{++} = (\rho e^2/k_B T)x_+^2z_+^2D_{++}$; and $\sigma_{+-} = (\rho e^2/k_B T)x_-x_+z_-z_+D_{+-}$. Physically, the distinct diffusivities D_{ij} quantify the slope of the long time correlated displacements of the distinct species i and j.

In general, computation of the distinct diffusion coefficients D_{ij} in simulations is extremely time-consuming and error prone and has very rarely been effected for polyIL systems.³¹ As a consequence, it has been common in many contexts to assume that the conductivity components σ_{-} and σ_{+} are representative of the overall conductivities and that the contributions σ_{ii} can be neglected. However, in the context of the present work, since the conductivity σ was measured from an independent nonequilibrium simulation framework involving the application of an electric field, the knowledge of σ and the self-diffusion coefficients $(D_+$ and $D_-)$ allows one to extract the distinct diffusivities D_{ij} , and thereby, the contributions σ_{ij} to the overall conductivity. We note that the results and discussion presented below pertain to our simulations in which the center of mass frame of reference was assumed to be stationary. For such a case, the distinct diffusion coefficients (D_{--}, D_{++}) and D_{+-}) are calculated by the following equations:

ACS Macro Letters

Letter

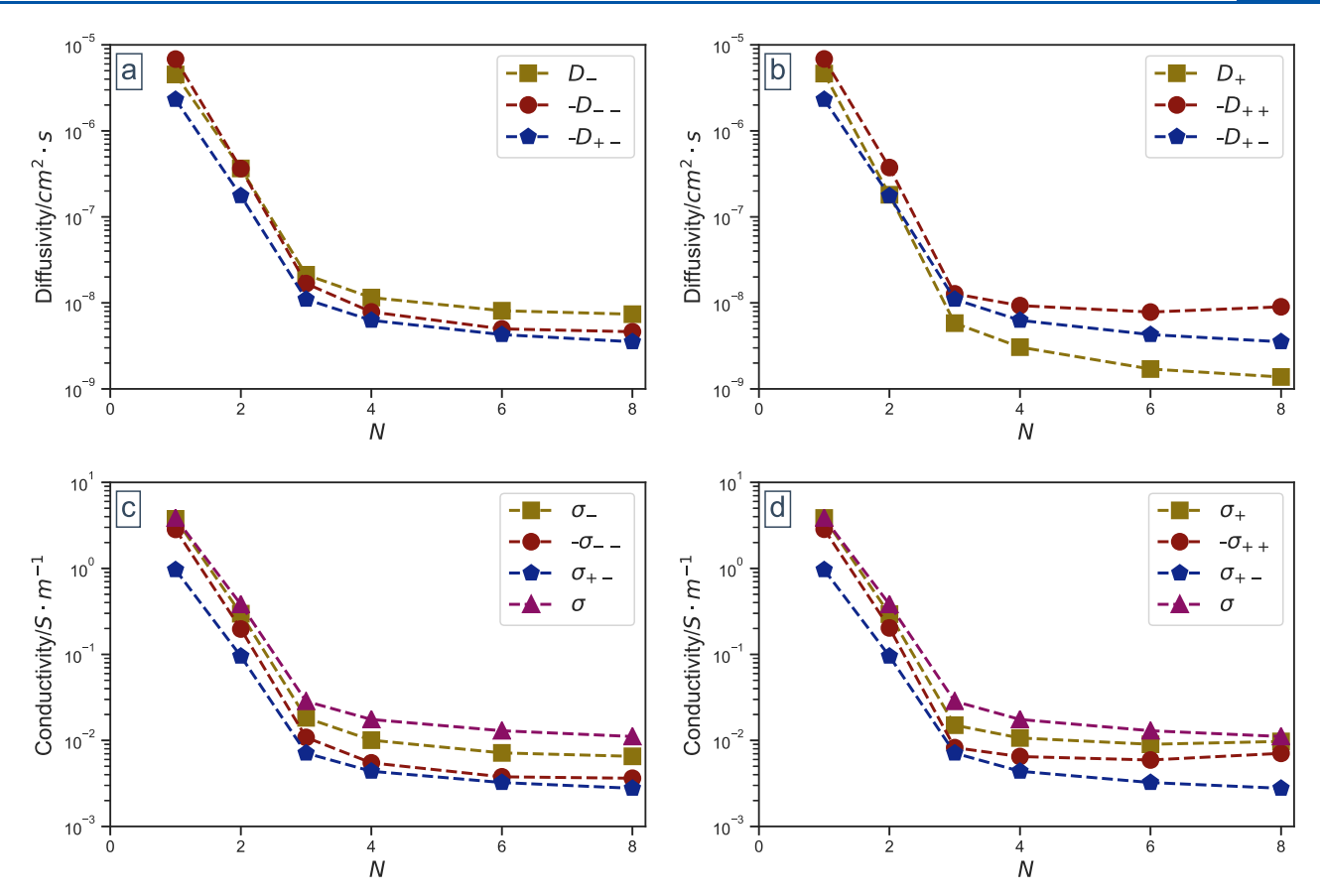


Figure 3. Self- and distinct-diffusion coefficients for anion (a) and cation (b) as a function of N, and the anion- (c) and cation-related (d) conductivity components as a function of N.

$$D_{--} = -\left[\frac{D_{-}}{x_{-}} - \frac{m_{+}^{2}\sigma}{(\rho e^{2}/k_{B}T)x_{-}^{2}[z_{+}m_{-} - z_{-}m_{+}]^{2}}\right]$$
(7a)

$$D_{++} = -\left[\frac{D_{+}}{x_{+}} - \frac{m_{-}^{2}\sigma}{(\rho e^{2}/k_{\rm B}T)x_{+}^{2}[z_{+}m_{-} - z_{-}m_{+}]^{2}}\right]$$
(7b)

$$D_{+-} = -\frac{m_{-}m_{+}\sigma}{(\rho e^{2}/k_{B}T)x_{-}x_{+}[z_{+}m_{-} - z_{-}m_{+}]^{2}}$$
(7c)

where σ is the true conductivity derived from the linear response regime under external electric fields, m_- and x_- are the mass and molar fraction for anion, m_+ and x_+ are the mass and molar fraction for cation, and ρ is the number density of the total charge carriers.

In Figure 3, we present the results for the different diffusion coefficients and their contributions to the conductivity. We observe that all the distinct diffusion coefficients are negative, indicating that their motions are anticorrelated and independent of whether the ion pair has the same or opposite charge. As a consequence, in Figure 3c,d, we see that the distinct anion—anion and distinct cation—cation correlated motions lead to a reduction in the conductivity relative to the ideal NE values. In contrast, the cation—anion correlated motions lead to an increase in conductivity relative to the ideal values. The latter result/observation is opposite to what is typically expected in salt-doped electrolyte systems but necessarily arises from physical constraints placed by the need for momentum to be conserved in polyILs s and molten salts.²⁷

To understand the mechanisms underlying the results noted in Figure 2b, we turn to the different contributions to the conductivity depicted in Figure 3c,d. We observe from Figure 3c, that with respect to the anions, the primary contribution to conductivity arises from self-diffusion (i.e., the "ideal" NE contribution). The correlated or distinct anion motions (σ_{--}) and the cation—anion correlations (σ_{-+}) are seen to contribute only a small portion to the overall conductivity. Together, such results suggest that conductivity contributions arising from the (distinct) anion—anion correlations and cation—anion correlations are small and not the origin of the results in Figure 2b.

From the results of Figure 3d, we observe that the conductivity contributions arising from the self-cation motion are comparable in magnitude to those arising from the selfanion motions. Moreover, for large N, the cation contributions are seen to exceed those of the anion (cf. SI, section S4, which explicitly displays a ratio of the σ_+ and σ_-). Such a trend is in contrast to the actual self-diffusivities of the anions and cations (Figures 1a and 3a,b), in which the cation self-diffusivities are an order of magnitude lower than the anions, and decreases more prominently with increasing N. To explain the apparent contrast with respect to the conductivity contributions, we note that the charge of the cation scales $z_{+} = N \cdot z_{-}$, and hence, the decrease in D_{+} is offset by the increased charge which accompanies the conductivity contributions. Such results explain the observation from Figure 2a that the ideal transference numbers of polyILs were close to 0.5 for smaller N and decreases with increasing N at larger N.

A second feature in Figure 3d is the magnitude of σ_{++} relative to σ_{+} and the overall conductivity. Explicitly, we

ACS Macro Letters Letter

observe that the conductivity contributions arising from the distinct cation—cation motions (σ_{++}) are comparable in magnitude (especially at high N) to the cation self-diffusivity's contribution to the conductivity. Such trends can in turn be traced back to the diffusivities displayed in Figure 3b, which demonstrate that the magnitudes of the correlated diffusivities D_{++} is significantly higher than the cation self-diffusivity D_{+} .

We do not have a conclusive explanation on the mechanistic origin of the above results relating to the diffusivity contributions arising from distinct cation-cation motions. We hypothesize that such results likely arise from the dynamical correlations between adjacent cations in the backbone of polyILs induced by the hopping motion of the anions. Indeed, as demonstrated in our previous articles, anion motion in such systems involve a correlated intramolecular hopping involving coordination with four cations from two different polymer backbones. 30,32,38 Such anion motions are likely to lead to strong dynamical correlations between the adjacent cations on the polymer backbone and those of the other polymer to which the anion is coordinated. We speculate that such correlations, which are inherently local in nature, results in distinct cation-cation diffusivities which are almost independent of N (at large N).

Additionally, we caution that the above results and discussion relating to the distinct diffusivities and conductivities are specific to the choice of the reference frame, which in this present study was chosen to be as one in which the center of mass of the system was assumed stationary. Other choices of the reference frame exist; in particular, the polymer itself may be a useful reference frame especially in the case of very high molecular weights. In SI (section S5), we present an elaborate discussion of the influence of the choice of reference frames, and the results for the case in which the center of mass of the polymer component alone is assumed stationary. The main conclusions arising therein are that the core results in the current paper, namely, the inverse Haven ratio H^{-1} and "ideal" transference number are independent from the choice of reference frame. For the case of a fixed polymer center of mass reference frame, we observe (cf. SI, Figure S10) that the conductivity contribution from the distinct cation-cation correlations remains an important aspect of the deviation from the ideal NE values.

Together our results and discussion above highlights that the dynamical correlations arising between distinct cations play a significant role in influencing the true conductivity of polyILs and thereby the inverse Haven ratio H^{-1} . Specifically, while almost all cation and anion distinct dynamical correlations decrease with increasing N, D_{++} is much larger than the selfcation contribution and becomes almost independent of N. As a consequence, σ_{++} increases with N at large N. Hence, the true conductivity is significantly smaller than the ideal NE value and results in the Haven ratio decreasing with increasing N. Due to computational limitations, we are unable to probe larger N, but note that, if we assume our trends continue to apply to higher MWs, our findings help rationalize the experimental results of Sokolov and co-workers in which they observed inverse Haven ratios of the order 10^{-2} for high molecular weight polyILs. 29

In summary, the results presented in this letter suggest that for polyILs, the inverse Haven ratio increases first with increasing degree of polymerization (N) and then decreases at larger N. We demonstrate that such results arise as a consequence of the strong cation—cation correlated motions, which exceed (in magnitude) the self-diffusivity of cations.

Further, we also provide evidence that the ideal transference numbers are not unity, but are instead influenced to a significant extent by the cationic contribution to the ideal conductivity. Together, our findings identify several new features relating to ion transport in polyILs and single ion conductors and challenge their promise as high transference number electrolytes.

ASSOCIATED CONTENT

S Supporting Information

The Supporting Information is available free of charge at https://pubs.acs.org/doi/10.1021/acsmacrolett.9b00908.

Section S1, the appendix for the derivation of the Nernst–Einstein conductivity for polyIL system; Section S2, the simulation details; Section S3, the fitting of diffusion coefficients D and ionic mobilities μ ; Section S4, the ratios of conductivity to the *true* conductivity σ ; Section S5, the center of mass of the polymer chains was chosen to be the reference frame and the corresponding distinct diffusivities and conductivities were calculated (PDF)

AUTHOR INFORMATION

Corresponding Author

*E-mail: venkat@che.utexas.edu.

ORCID 🏻

Zidan Zhang: 0000-0002-6909-8742 Bill K. Wheatle: 0000-0003-0550-4905 Jakub Krajniak: 0000-0001-9372-6975 Jordan R. Keith: 0000-0003-2639-3087 Venkat Ganesan: 0000-0003-3899-5843

Notes

The authors declare no competing financial interest.

ACKNOWLEDGMENTS

The authors work on the topic of ion transport in polymer electrolytes have been generously supported by grants from Robert A. Welch Foundation (Grant F1599) and the National Science Foundation (CBET-17069698 and DMR-1721512). The development of the nonequilibrium simulation methodology for ion conductivities was supported as part of the Center for Materials for Water and Energy Systems, an Energy Frontier Research Center funded by the U.S. Department of Energy, Office of Science, Basic Energy Sciences under Award #DE-SC0019272. The authors acknowledge the Texas Advanced Computing Center (TACC) for the generous allocation of computing resources. We thank Prof. Nitash Balsara for illuminating discussions on the definition of transference numbers.

REFERENCES

- (1) Zhu, Y. S.; Wang, X. J.; Hou, Y. Y.; Gao, X. W.; Liu, L. L.; Wu, Y. P.; Shimizu, M. A new single-ion polymer electrolyte based on polyvinyl alcohol for lithium ion batteries. *Electrochim. Acta* **2013**, *87*, 113–118.
- (2) Porcarelli, L.; Shaplov, A. S.; Bella, F.; Nair, J. R.; Mecerreyes, D.; Gerbaldi, C. Single-Ion Conducting Polymer Electrolytes for Lithium Metal Polymer Batteries that Operate at Ambient Temperature. ACS Energy Letters 2016, 1, 678–682.
- (3) Zhang, H.; Li, C.; Piszcz, M.; Coya, E.; Rojo, T.; Rodriguez-Martinez, L. M.; Armand, M.; Zhou, Z. Single lithium-ion conducting

ACS Macro Letters Letter

solid polymer electrolytes: advances and perspectives. *Chem. Soc. Rev.* **2017**, *46*, 797–815.

- (4) Qian, W.; Texter, J.; Yan, F. Frontiers in poly(ionic liquid)s: syntheses and applications. *Chem. Soc. Rev.* **2017**, *46*, 1124–1159.
- (5) Porcarelli, L.; Manojkumar, K.; Sardon, H.; Llorente, O.; Shaplov, A. S.; Vijayakrishna, K.; Gerbaldi, C.; Mecerreyes, D. Single Ion Conducting Polymer Electrolytes Based On Versatile Polyurethanes. *Electrochim. Acta* **2017**, 241, 526–534.
- (6) Ganesan, V. Ion transport in polymeric ionic liquids: recent developments and open questions. *Molecular Systems Design & Engineering* **2019**, *4*, 280–293.
- (7) LaFemina, N. H.; Chen, Q.; Mueller, K. T.; Colby, R. H. Diffusive Flux as a New Metric for Ion-Conducting Soft Materials. *ACS Energy Letters* **2016**, *1*, 1179–1183.
- (8) Ohno, H.; Ito, K. Room-Temperature Molten Salt Polymers as a Matrix for Fast Ion Conduction. *Chem. Lett.* **1998**, *27*, 751–752.
- (9) Ohno, H. Molten salt type polymer electrolytes. *Electrochim. Acta* **2001**, *46*, 1407–1411.
- (10) Yuan, J.; Mecerreyes, D.; Antonietti, M. Poly(ionic liquid)s: An update. *Prog. Polym. Sci.* **2013**, *38*, 1009–1036.
- (11) Choi, J.-H.; Ye, Y.; Elabd, Y. A.; Winey, K. I. Network Structure and Strong Microphase Separation for High Ion Conductivity in Polymerized Ionic Liquid Block Copolymers. *Macromolecules* **2013**, 46, 5290–5300.
- (12) Shaplov, A. S.; Ponkratov, D. O.; Aubert, P.-H.; Lozinskaya, E. I.; Plesse, C.; Vidal, F.; Vygodskii, Y. S. A first truly all-solid state organic electrochromic device based on polymeric ionic liquids. *Chem. Commun.* **2014**, *50*, 3191–3193.
- (13) Yu, Y.; Lu, F.; Sun, N.; Wu, A.; Pan, W.; Zheng, L. Single lithium-ion polymer electrolytes based on poly(ionic liquid)s for lithium-ion batteries. *Soft Matter* **2018**, *14*, 6313–6319.
- (14) Ohno, H. Functional Design of Ionic Liquids. *Bull. Chem. Soc. Jpn.* **2006**, *79*, 1665–1680.
- (15) Matsumi, N.; Sugai, K.; Miyake, M.; Ohno, H. Polymerized Ionic Liquids via Hydroboration Polymerization as Single Ion Conductive Polymer Electrolytes. *Macromolecules* **2006**, *39*, 6924–6927.
- (16) Mecerreyes, D. Polymeric ionic liquids: Broadening the properties and applications of polyelectrolytes. *Prog. Polym. Sci.* **2011**, *36*, 1629–1648.
- (17) Nishimura, N.; Ohno, H. 15th anniversary of polymerised ionic liquids. *Polymer* **2014**, *55*, 3289–3297.
- (18) Kim, T. Y.; Lee, H. W.; Stoller, M.; Dreyer, D. R.; Bielawski, C. W.; Ruoff, R. S.; Suh, K. S. High-Performance Supercapacitors Based on Poly(ionic liquid)-Modified Graphene Electrodes. *ACS Nano* **2011**, *5*, 436–442.
- (19) Wang, Y.; Agapov, A. L.; Fan, F.; Hong, K.; Yu, X.; Mays, J.; Sokolov, A. P. Decoupling of Ionic Transport from Segmental Relaxation in Polymer Electrolytes. *Phys. Rev. Lett.* **2012**, *108*, 88303.
- (20) Fan, F.; Wang, Y.; Hong, T.; Heres, M. F.; Saito, T.; Sokolov, A. P. Ion Conduction in Polymerized Ionic Liquids with Different Pendant Groups. *Macromolecules* **2015**, *48*, 4461–4470.
- (21) Fan, F.; Wang, W.; Holt, A. P.; Feng, H.; Uhrig, D.; Lu, X.; Hong, T.; Wang, Y.; Kang, N.-G.; Mays, J.; Sokolov, A. P. Effect of Molecular Weight on the Ion Transport Mechanism in Polymerized Ionic Liquids. *Macromolecules* **2016**, *49*, 4557–4570.
- (22) Frenzel, F.; Guterman, R.; Anton, A. M.; Yuan, J.; Kremer, F. Molecular Dynamics and Charge Transport in Highly Conductive Polymeric Ionic Liquids. *Macromolecules* **2017**, *50*, 4022–4029.
- (23) Griffin, P. J.; Freyer, J. L.; Han, N.; Geller, N.; Yin, X.; Gheewala, C. D.; Lambert, T. H.; Campos, L. M.; Winey, K. I. Ion Transport in Cyclopropenium-Based Polymerized Ionic Liquids. *Macromolecules* **2018**, *51*, 1681–1687.
- (24) Fong, K. D.; Self, J.; Diederichsen, K. M.; Wood, B. M.; McCloskey, B. D.; Persson, K. A. Ion Transport and the True Transference Number in Nonaqueous Polyelectrolyte Solutions for Lithium Ion Batteries. ACS Cent. Sci. 2019, 5, 1250–1260.
- (25) Wieland, F.; Bocharova, V.; Münzner, P.; Hiller, W.; Sakrowski, R.; Sternemann, C.; Böhmer, R.; Sokolov, A. P.; Gainaru, C. Structure

and dynamics of short-chain polymerized ionic liquids. *J. Chem. Phys.* **2019**, *151*, 34903.

- (26) Harris, K. R. Relations between the Fractional Stokes-Einstein and Nernst-Einstein Equations and Velocity Correlation Coefficients in Ionic Liquids and Molten Salts. *J. Phys. Chem. B* **2010**, *114*, 9572–9577.
- (27) Kashyap, H. K.; Annapureddy, H. V. R.; Raineri, F. O.; Margulis, C. J. How Is Charge Transport Different in Ionic Liquids and Electrolyte Solutions? *J. Phys. Chem. B* **2011**, *115*, 13212–13221.
- (28) Zhang, Y.; Maginn, E. J. Direct Correlation between Ionic Liquid Transport Properties and Ion Pair Lifetimes: A Molecular Dynamics Study. *J. Phys. Chem. Lett.* **2015**, *6*, 700–705.
- (29) Stacy, E. W.; Gainaru, C. P.; Gobet, M.; Wojnarowska, Z.; Bocharova, V.; Greenbaum, S. G.; Sokolov, A. P. Fundamental Limitations of Ionic Conductivity in Polymerized Ionic Liquids. *Macromolecules* **2018**, *51*, 8637–8645.
- (30) Keith, J. R.; Mogurampelly, S.; Aldukhi, F.; Wheatle, B. K.; Ganesan, V. Influence of molecular weight on ion-transport properties of polymeric ionic liquids. *Phys. Chem. Chem. Phys.* **2017**, *19*, 29134—29145.
- (31) Mogurampelly, S.; Ganesan, V. Ion Transport in Polymerized Ionic Liquid-Ionic Liquid Blends. *Macromolecules* **2018**, *51*, 9471.
- (32) Zhang, Z.; Krajniak, J.; Keith, J. R.; Ganesan, V. Mechanisms of Ion Transport in Block Copolymeric Polymerized Ionic Liquids. *ACS Macro Lett.* **2019**, *8*, 1096–1101.
- (33) Ratkje, S. K.; Rajabu, H.; Førland, T. Transference coefficients and transference numbers in salt mixtures relevant for the aluminium electrolysis. *Electrochim. Acta* **1993**, *38*, 415–423.
- (34) Harris, K. R. Comment on "Negative effective Li transference numbers in Li salt/ionic liquid mixtures: does Li drift in the "Wrong" direction?" by M. Gouverneur, F. Schmidt and M. Schönhoff, Phys. Chem. Chem. Phys., 2018, 20, 7470. Phys. Chem. Chem. Phys. 2018, 20, 30041–30045.
- (35) Matsunaga, S.; Koishi, T.; Tamaki, S. Velocity correlation functions and partial conductivities of molten AgI–AgBr by molecular dynamics simulation. *Mater. Sci. Eng., A* **2007**, 449–451, 693–698.
- (36) Tu, K.-M.; Ishizuka, R.; Matubayasi, N. Spatial-decomposition analysis of electrical conductivity in ionic liquid. *J. Chem. Phys.* **2014**, 141, 244507.
- (37) Jorgensen, W. L.; Maxwell, D. S.; Tirado-Rives, J. Development and Testing of the OPLS All-Atom Force Field on Conformational Energetics and Properties of Organic Liquids. *J. Am. Chem. Soc.* **1996**, 118, 11225–11236.
- (38) Mogurampelly, S.; Keith, J. R.; Ganesan, V. Mechanisms Underlying Ion Transport in Polymerized Ionic Liquids. *J. Am. Chem. Soc.* **2017**, *139*, 9511–9514.
- (39) Lee, S. H.; Rasaiah, J. C. Molecular dynamics simulation of ionic mobility. I. Alkali metal cations in water at 25 °C. *J. Chem. Phys.* **1994**, *101*, 6964–6974.
- (40) Ting, C. L.; Stevens, M. J.; Frischknecht, A. L. Structure and Dynamics of CoarseGrained Ionomer Melts in an External Electric Field. *Macromolecules* **2015**, *48*, 809–818.
- (41) Alshammasi, M. S.; Escobedo, F. A. CorrelationbetweenIonicMobilityandMicrostructure in Block Copolymers. A Coarse-Grained Modeling Study. *Macromolecules* **2018**, *51*, 9213–9221.